Arabian Journal of Chemistry (2019) **12**, 1595–1606

King Saud University

Arabian Journal of Chemistry

www.ksu.edu.sa
www.sciencedirect.com

SPECIAL ISSUE: ENVIRONMENTAL CHEMISTRY

Kinetics and isotherm studies of methyl orange adsorption by a highly recyclable immobilized polyaniline on a glass plate

K. Haitham, S. Razak, M.A. Nawi *

School of Chemical Sciences, Universiti Sains Malaysia, 11800 Penang, Malaysia

Received 22 February 2013; accepted 8 October 2014
Available online 23 October 2014

KEYWORDS

Immobilized polyaniline;
Methyl orange;
Reusable;
Photocatalytic regeneration;
Wastewater treatment

Abstract Immobilized polyaniline on glass plates (PANI/glass) and its powder form were compared for the adsorption of methyl orange (MO) dye from aqueous solutions. The effects of operational parameters such as pH, sorbent dosage, initial concentration, contact time, aeration rate and the thermodynamics of the uptake of MO had been exhaustively evaluated. The maximum adsorption capacity (q_{max}) for PANI/glass and PANI powder was 93 and 147 mg g^{-1}, respectively. In addition, pseudo-second order model was the best fitted kinetic model for both systems, suggesting that the rate-limiting step may be chemisorptions. The obtained negative values of free energy and enthalpy indicated the adsorption process was spontaneous and exothermic. In contrast to PANI powder, PANI/glass yielded negative entropy. Photocatalytic regeneration of used PANI/glass was found to be highly effective where the desorbed MO was completely mineralized. This study showed that immobilized PANI offered the unique advantage of convenient use and reuse over an extended period of applications.
© 2014 The Authors. Production and hosting by Elsevier B.V. on behalf of King Saud University. This is an open access article under the CC BY-NC-ND license (http://creativecommons.org/licenses/by-nc-nd/3.0/).

1. Introduction

Many industries often use dyes and pigments to color their products. Even though some dyes are non-toxic and inert at the concentration discharged into the receiving water however, they impart color undesirable to the water users (Ayad and Abu El Nasr, 2010). In addition, the presence of coloring material in the water system also reduces penetration of light and thereby affecting photosynthesis of the aquatic vegetations (Mittal et al., 2007). In this light, considerable attention has been paid to adsorption technologies for developing an efficient and sufficient method for removing dyes from the wastewater effluents (Qin et al., 2009). Many effective and cheaper adsorbent materials have been developed such as chitosan beads (Cestari et al., 2004), sludge ash (Weng and Pan, 2006), hazelnut shell (Dogan et al., 2009), soya oil and bottom ash (Mittal et al., 2007), silica (Krysztafkiewicz et al., 2002), titania aerogel (Abramian and El-Rassy, 2009), modified peat (Sun and Yang, 2003), banana, orange peels (Annadurai et al.,

* Corresponding author. Tel.: +60 4 6534031; fax: +60 4 6574854.
E-mail address: masri@usm.my (M.A. Nawi).
Peer review under responsibility of King Saud University.

Production and hosting by Elsevier

http://dx.doi.org/10.1016/j.arabjc.2014.10.010
1878-5352 © 2014 The Authors. Production and hosting by Elsevier B.V. on behalf of King Saud University.
This is an open access article under the CC BY-NC-ND license (http://creativecommons.org/licenses/by-nc-nd/3.0/).

2002) and so on. Recently, polyaniline (PANI) has received a great deal of attention (Ai et al., 2010) due to its unique electrical property, good environmental stability and easy and economical preparation methods (Ayad and Abu El Nasr, 2010; Palaniappan and John, 2008; Bhadra et al., 2009). Aniline polymerization in an aqueous acidic medium yields the most conductive form of PANI, the emeraldine salt (ES) which is converted to the corresponding emeraldine base (EB) by treatment with an alkaline solution or by rinsing with a large excess of water (Ayad and Abu El Nasr, 2010).

Recently, PANI microspheres were synthesized by a facile solution route in the acidic medium to remove MO (Ai et al., 2010). Ansari and Mosayebzadeh (2011) used particles of sawdust surface coated with PANI to remove an anionic dye. Gemeay et al. (2008) developed PANI/MnO_2 composites for the oxidative decolorization of direct red 81 (DR-81), indigo carmine (IC), and acid blue 92 (AB-92) in the presence H_2O_2. The kinetics of direct blue 78 removals from aqueous solution by PANI salt powder have been studied by Salem (2010) whereby the removal rate was found to depend largely on the activity of the polymer salts. PANI had also been reported to be a good adsorbent for the removal of some metal ions such as Cr (VI) (Samani et al., 2010), Cr (III) (Kumar et al., 2008), Hg (Cui et al., 2012), F (Karthikeyan et al., 2009), Cu (Chen et al., 2011) and Cd (Mansour et al., 2011).

Even though PANI has been proven to be a good adsorbent, in most cases, PANI or its composites had been applied in suspended form which required filtration of the treated water and recovery of the nano PANI adsorbent. On the other hand, the immobilized PANI/glass system would be expected to offer many advantages from an environmental point of view such as a long-term reusability, elimination of the need to filter the treated water, and easy storage. Another advantage of this immobilized mode is the simple recovery of dyes and regeneration of the adsorbent which could be difficult for the conventionally used powder form of PANI (Ansari and Mosayebzadeh, 2011).

The objective of this work was to fabricate and characterize immobilized PANI on glass plates (PANI/glass) for the removal of anionic dye from aqueous solution. The second objective was to compare this unique adsorbent plate against the conventional PANI powder form in terms of the adsorption kinetics, isotherm and thermodynamic characteristics. The third objective was to study the reusability of the immobilized PANI/glass plate which also included its regeneration process.

2. Experimental

2.1. Materials

The aniline liquid (C_6H_7N) was purchased from Sigma – Aldrich while methyl orange (MO) with 50% dye content was provided by Aldrich. Its stock solution was prepared in ultra pure water and was diluted to the desired concentrations. Ammonium peroxydisulfate (APS) and the surfactant polyvinylpyrrolidone (PVP) were both from Aldrich. All chemicals were used as received.

2.2. Preparation and immobilization of PANI

PANI was prepared based largely on the methods of Blinova et al. (2005) and Somani (2002) with some modifications. The chemical oxidative polymerization of PANI (Emeraldine salt) was carried out in an aqueous acidic solution of 0.06 M aniline and 25 ml of 0.5 M H_2SO_4 at room temperature. 1 g of polyvinylpyrrolidone (PVP) was added to the solution to enhance the solubility of the polymer and also to act as adhesive during its immobilization on the glass substrate. Then 0.06 M of $(NH_4)_2S_2O_8$ (APS) in 25 ml of 0.5 M H_2SO_4 was added under constant stirring for 10 h.

The glass plates (with ground surface on one of its sides), each of dimension 4.7×6.5 cm were first cleaned by sonication in water followed by washing in acetone and ultra pure water then dried in the oven for about 10 min after which the weight of each glass plate was taken. About 20 mL PANI solution was poured into a coating cell of dimension $6.0\ \text{cm} \times 8.0\ \text{cm} \times 0.5$ cm. The glass plate was then immersed vertically for a few seconds in the solution so that only the top 2 cm of the plate remained uncoated. The coated glass plate was then pulled slowly out of the coating cell and dried using a hair drier to yield a layer of PANI on both sides of the glass. The previous steps can be repeated in order to increase the thickness or loading of the immobilized PANI. The PANI layer coated on the smooth side of the glass plate was then scrapped off. The fabricated immobilized PANI was termed as PANI/glass plate. All PANI/glass plates were conditioned in distilled water for 30 min prior to use to remove the acidic by-products of polymerization reaction. PANI powder was obtained by drying the PANI solution in an oven at 60 °C for 24 h after which it was washed and filtered repeatedly with distilled water. After drying, it was grinded with mortar, sieved ($\leqslant$150 μm) and kept in a tightly capped amber bottle.

2.3. Characterization of PANI

Brunauer, Emmet and Teller (BET) surface area was measured using Quantachrome autosorb automated gas sorption system. Scanning electron microscope (SEM-EDX, Model Leica Cambridge S360) was used to observe the surface morphology of PANI and the thickness of the immobilized PANI layer. X-ray diffraction system, Model, Panalytical X pert Pro MRD PW3040 was used to determine the crystal phase of PANI. The FT-IR spectra were observed using an FT-IR System 2000 Model spectrometer within 400–4000 cm^{-1}. UV–vis diffuse reflectance spectroscopy (DRS) was carried out via a Perkin–Elmer, Lambda 35 UV–vis spectrometer. The spectrum was recorded in the wavelength range of 300–900 nm.

2.4. Batch adsorption experiments

The experimental set-up for the adsorption study was relatively unique in order to accommodate the flat PANI/glass plate which mimics the water baffle system that is commonly used in industrial and municipal waste water treatment. The experiments with immobilized and powder form were conducted using the reactor as shown in Fig. 1. The reactor is a custom made cell of dimension $6\ \text{cm} \times 8\ \text{cm} \times 1$ cm that can hold up to 20 mL of solution. An aquarium pump aerator

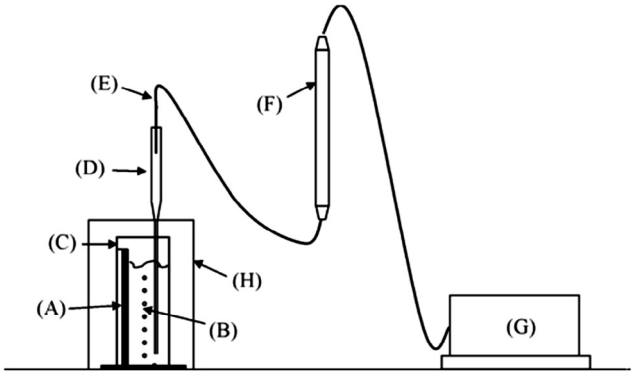

Figure 1 Schematic of the batch adsorption of MO by PANI/glass (A) PANI/glass, (B) MO aqueous solution, (C) glass container, (D) Pasteur pipette, (E) PVC tube, (F) air flow meter, (G) aquarium pump, and (H) box.

was attached to the container via PVC tubing for supply of air and agitation of the solution.

For batch adsorption experiments, the PANI/glass plate was placed uprightly inside the cell after which it was filled with 20 mL MO solution. Aeration was carried out throughout the adsorption process to provide proper agitation of the solution for solute transport purposes (Nawi and Zain, 2012). To determine the optimum conditions for the dye sorption, various operational parameters were carried out such as adsorbent dosage (0.26–2.06 mg cm^{-1}), pH (3–11), contact time (1–90 min), initial dye concentration (5–30 mg L^{-1}), aeration rate (0–140 ml min^{-1}) and temperature (300–340 K). The pH of MO solution was adjusted by adding either 0.10 M HCl or NaOH. A water bath was used to control the temperature. A HACH DR/2000 Direct Reading Spectrophotometer at a wavelength of 464 nm was used to monitor the concentrations of MO at a different time interval. Under acidic conditions, wavelength of 508 NM was used instead.

The adsorption capacity at equilibrium, q_e (mg g^{-1}), was calculated using the following equation:

$$q_e = \frac{(C_o - C_e)V}{m} \quad (1)$$

where C_o is the initial dye concentration (mg L^{-1}), C_e is the dye concentration at equilibrium (mg L^{-1}), V is the volume of dye solution used (L), and m is the mass of the adsorbent used (mg). The percentage of removal (% R) of MO is defined as:

$$\%R = \frac{(C_o - C_e)}{C_o} 100 \quad (2)$$

where C_o and C_e are the initial and the equilibrium dye concentrations (mg L^{-1}), respectively. Adsorption experiments were repeated three times in order to achieve better precision and the results are reported as average values.

2.5. Reusability and photocatalytic regeneration of PANI/glass plates

For reusability study, a single plate was used repeatedly for the adsorption of MO. For this purpose, a 20 mL, 60 mg L^{-1} MO solution was used in the presence of a PANI/glass plate as described earlier with a contact time of 1 h and aeration rate of 40 mL min^{-1}. Upon completion of the first cycle, the used PANI/glass plate was rinsed thoroughly and reused for the second cycle of adsorption of 60 mg L^{-1} MO solution. The cycles of reuse of the same plate were carried out for a total of 5 cycles. The percent removal MO was then calculated for each cycle of reuse.

After the fifth cycle, the used PANI/glass plate was photocatalytically regenerated using a 45 Watt Phillips ecotone compact fluorescent lamp light source. To the reactor containing the used PANI/glass plate was added 20 mL of 0.005 M H_2SO_4 (pH 2). After a thorough mixing via aeration, 0.02 g P-25 TiO_2 powder was added together with 50 μL 37% H_2O_2. The cell was then irradiated for 3 h until the color of the solution became almost colorless after which it was discharged into a beaker. Then a 20 mL solution of 0.5 M H_2SO_4 was added to the reactor together with 0.02 g P-25 TiO_2 powder and 50 μL 37% H_2O_2 and again irradiated for another 4 h until the solution became colorless. The treated acidic solution was then discharged and combined with the previous solution for a further irradiation (without PANI/glass plate) for another 4 h in order to complete the mineralization process of the desorbed MO dye. The total organic carbon (TOC) of the treated solution was measured using the Shimadzu H561048 TOC analyzer. The regenerated PANI/glass plate was then rinsed with water and reused again for another 5 cycles of applications to adsorb 60 mg L^{-1} MO solution as described earlier.

3. Results and discussion

3.1. Characterization of immobilized PANI/glass system

Several workers had synthesized PANI in the presence of PVP in order to produce a finely dispersed PANI in solution (Blinova et al., 2005; Somani, 2002). In fact a brief description of the role of PVP in PANI synthesis had been properly described by Murugesan et al., 2004. However, no one has taken advantage of the added PVP as adhesive for immobilizing PANI on solid supports. In this study, we had utilized PVP as the adhesive for immobilizing PANI on glass plates and evaluated its adsorptive properties of MO.

Fig. 2a shows the IR spectrum of immobilized PANI (PANI/glass) in the range of 4000–400 cm^{-1}. The adsorption bands at 1581 and 1493 cm^{-1} are assigned to the C═C stretching vibration of the quinoid ring and the benzenoid ring (Ren et al., 2009). The peaks at 1373 and 1301 cm^{-1} correspond to C—N and C═N stretching modes (Palaniappan et al., 2011) while the peak at 1137 cm^{-1} is assigned to the C—H in plane deformation (Choudhury, 2009). The peak at 820 cm^{-1} can be attributed to the out-of-plane C—H bending modes (Eisazadeh et al., 2010) and the absorption band assignable to C═O is observed at 1638 cm^{-1} which indicates the presence of PVP (Feng et al., 2006).

The diffuse reflectance UV–vis spectrum (DRS) of the PANI/glass is shown in Fig. 2b. PANI has three distinct absorption peaks around 291, 377 and a broad peak at 643 which are associated with a π–π^* benzenoid transition rings, polaron band and π–π^* quinoid transition rings, respectively (Mahanta et al., 2008). The polaron band transition is a typical absorption band of doped PANI therefore the prepared PANI/glass was in doped state (Ren et al., 2009).

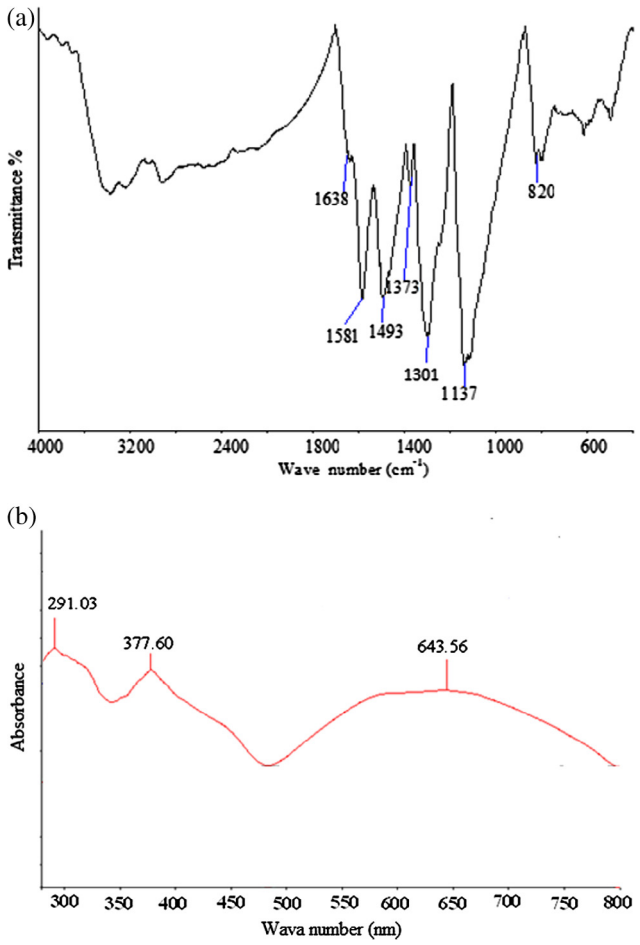

Figure 2 Spectral analysis of PANI (ES): (a) FT-IR spectra and (b) UV–vis DRS spectra.

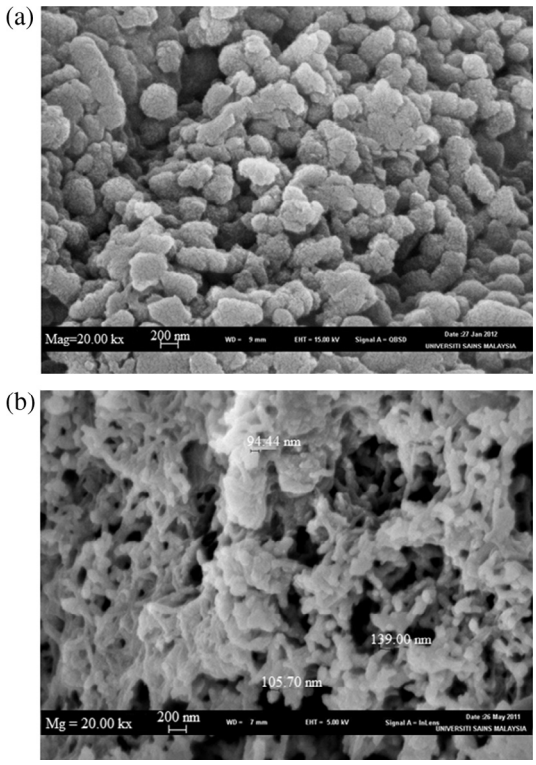

Figure 3 SEM micrographs of: (a) PANI powder and (b) PANI/glass.

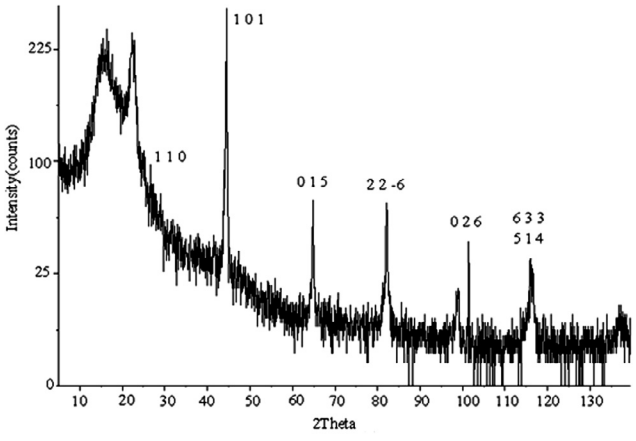

Figure 4 XRD pattern of PANI synthesized by the chemical oxidation polymerization.

The SEM micrographs of PANI powder and PANI/glass are shown in Fig. 3a and b, respectively. It can be seen that the surface morphology of PANI powder was composed of irregular agglomerates of nanoparticles. On the other hand, PANI/glass aggregates have irregular diameter between 86 and 158 nm which merge tightly with each other to exhibit a netlike macro porous state. This macro porous structure of the immobilized PANI is expected to contribute to the efficient adsorption of adsorbates since it provides a path for the insertion and extraction of molecules or ions within the inner layer of the immobilized adsorbent. The thickness of the immobilized PANI would depend on the amount of PANI loading on the glass plate. The measurement of the thickness of the immobilized PANI layers was done via SEM analyses. The immobilized PANI layer increased from 7.35 ± 0.15 to 35.0 ± 0.11 μm with the increase of adsorbent loading from 0.27 mg cm^{-2} to 2.06 mg cm^{-2} (see Supplementary Fig. 1).

The amorphous nature of PANI was confirmed by the energy-dispersive X-ray analysis (EDX) pattern. As seen in Fig. 4, there are many sharp peaks in the range of 10–130 2θ. The broad peak with 2θ around 23.2° is related to the diffraction of amorphous PANI (Jing et al., 2007). The peaks at $2\theta = 22$, 64, and 82 belong to the sulfuric acid entities. The other peaks around $2\theta = 44$ and 116 are related to hydrogen and sulfur. The presence of sulfur is partly due to the residual sulfate counter ions produced by the reduction of peroxydisulfate during polymerization (Stejskal and Gilbert, 2002).

The BET surface area (S_{BET}) for both PANI powder and PANI/glass is given in Table 1. S_{BET} for PANI powder in this study was 11.8 $m^2\ g^{-1}$. This is relatively smaller than the S_{BET} values reported in other works (Nand et al., 2011; Supri and Heah, 2010; He, 2005). The smaller S_{BET} value was probably caused by the presence of PVP which was added as emulsifier and adhesive during the synthetic process. As expected, immobilization caused a decrease in the BET surface area of the adsorbent from 11.8 to 3.7 $m^2\ g^{-1}$. The nitrogen adsorption–desorption isotherms (see Supplementary Fig. 2) indicated that

Table 1 BET surface areas and the Langmuir and Freundlich isotherms parameters for the adsorption of MO by PANI/glass and PANI powder [volume: 0.02 L, time: 60 min, mass: 0.94 mg cm^{-2} (PANI/glass), 20 mg (PANI powder) and Temp: 29 °C].

Adsorbent	Langmuir				Freundlich			S_{BET}
	K_L (L g^{-1})	a_L (L mg^{-1})	q_{max} (mg g^{-1})	R^2	n_F	K_F (L g^{-1})	R^2	(mg m^{-2})
PANI/glass	175.439	1.912	91.743	0.920	1.484	57.077	0.975	3.7
PANI powder	144.928	0.986	147.059	0.994	1.753	69.616	0.965	11.8

it was of type II meaning that the synthesized PANI powder was a non porous solid.

3.2. Adsorption of methyl orange by PANI/glass plate

The adsorption of MO by the PANI/glass was done in the presence of aeration. This is in direct contrast to the conventional set up of adsorption process which is normally done under stirring or shaking. We have taken this approach for two reasons. The main reason was to mimic the set up of our photocatalytic system (Nawi and Zain, 2012) so that obtained adsorption data would be useful when a bilayer system of PANI/TiO_2 was to be fabricated later in future studies. Secondly, it has been proven by Jia et al. (2005, 2006) that aeration was a more favorable approach than the normal stirring mode when they concluded that it enhanced the adsorption of a dilute organic solute onto powdered activated carbon (PAC). This phenomenon was due to the mass transfer coefficient in the liquid film surrounding the PAC that increased linearly with the increase of aeration rate. Therefore this approach should be a better way of providing the mass transport of dyes to the vertically placed adsorbent plate used in this study.

In order to determine the effect of aeration on the MO adsorption by the PANI/glass plate, a series of studies involving stirring (no aeration) and aeration at different rates were carried out. As shown in Fig. 5, the adsorption capacity (q_e) increased with aeration rate until 40 ml min^{-1}. Beyond this value, the adsorption capacity remained more or less constant. Under this condition, the adsorption capacity was found to be higher than the system carried out under stirring. The constant value of q_e obtained beyond aeration rate of 40 ml min^{-1} indicated that this flow rate should be the optimum aeration flow rate since optimum mass transfer had been attained for the maximum adsorption of MO.

Contrary to the conventional suspended type adsorption study involving powdered adsorbents, the thickness of the immobilized adsorbent would be an important parameter that may influence the uptake of the adsorbates. The immobilized PANI thickness would depend on the PANI loading on the glass substrates. Various PANI/glass with different PANI loadings were fabricated using a series of identical size glass plates with dry weights of immobilized PANI ranging from 0.27 mg cm^{-2} to 2.06 mg cm^{-2}. These respective plates were then exposed to a fixed concentration of MO dye solution. As observed in Fig. 6, the percentage removal of MO dye increased with the thickness or the loading of the immobilized PANI until the loading reached 0.47 mg cm^{-2} (or 10 mg) where the percent MO removed was already 100%. The adsorption capacity, q_e (mg g^{-1}), however, decreased with the increasing load or thickness. The explanation for this was that at the PANI loading greater than 0.47 mg cm^{-2}, there would be excess of adsorption sites due to the fixed concentration of MO used in the adsorption study. In other words, increasing the loading or thickness of PANI beyond 0.47 mg cm^{-2} would increase unused available site within the immobilized PANI thus reducing the value of the adsorption capacity. What had been observed was indeed very similar to the behavior of adsorption of anionic sulphonated Acid Red 14 (AR) dye by the PANI powder (Sahar et al., 2012). This implies that the mass transport of MO dye was not significantly affected by the thickness of the immobilized PANI. This was due to the presence of macropores within the network like

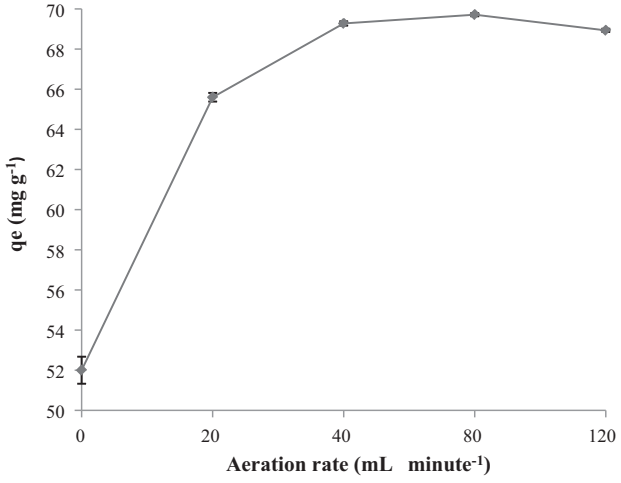

Figure 5 Effect of aeration rates on the adsorption capacity of MO onto PANI/glass [V: 0.02 L, t: 90 min, m: 1.41 mg cm^{-2}, pH: solution (7.0), C_o: 20 mg L^{-1} and T: 29 °C].

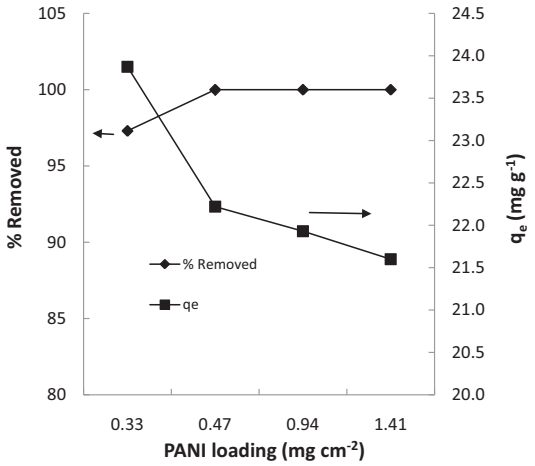

Figure 6 Effect of different PANI/glass loadings on the adsorption capacity and percentage remaining of MO [V: 0.02 L, t: 90 min, pH: solution (7.0), C_o: 20 mg L^{-1}, and T: 29 °C].

structure of the immobilized PANI (Fig. 3) which provided an easy path for the insertion and extraction of molecules or ions within the inner layer of the immobilized adsorbent. On the other hand, for the case of immobilized CS (Nawi et al., 2010), both percentage removal and adsorption capacity for RR4 dye decreased with the loading or thickness of chitosan. According to Nawi et al. (2010), this was due to the mass transfer difficulty with the increased thickness since CS layer became more compact with increasing thickness where the pores actually decreased with depth. The fact that immobilized PANI yielded the curves shown in Fig. 6 which was similar to PANI powder affirmed the contribution of the network structures in allowing the easy mass transport of the MO dye within the immobilized layer.

pH is the most important factor affecting the adsorption process. The effect of pH on the adsorption of MO by the immobilized PANI/glass plate at initial pH values ranging from 3 to 11 is shown in Fig 7. Adsorption capacity was at maximum values when the initial pH was from 4 to 8. The value of q_e decreased upon increasing or decreasing the initial pH values of the solutions from this range of pH values. This behavior can be explained by the effect of pH on the MO molecules and its effect on the surface of adsorbent. It is obvious that the degree of ionization of a dye molecule depends on the pH of the aqueous medium. MO contains one sulfonate group ($-SO_3Na$) and its pK_a is 3.8 (Comparelli et al., 2005). At neutral pH, a significant amount of MO would be in the anionic form. The other functional group is the amine group which would be uncharged under neutral and alkaline conditions. When the pH was adjusted to acidic condition, the amine functional group of MO molecules would begin to be protonated and the negative charge density would be reduced while the positive charge density would increase due to the protonation of the nitrogen atom and sulfonate groups. Therefore at pH 3, MO dyes would be positively charged. The surface of PANI is also affected by pH whereby under acidic condition (ES form) it would be positively charged while under alkaline condition (EB form), it would be uncharged. According to Kuramoto and Geniès (1995) the transition from the ES (positively charged) form to the EB form (negatively charged) occurs at pH 7–8. Therefore, at pH 3, PANI would exist in the ES form and was positively charged. As shown in Fig. 7, the adsorption capacity q_e (13 mg g^{-1}) at pH 3 was relatively low since some electrostatic repulsion would occur between the MO molecules and the positively charged surface of PANI. The limited adsorption at pH 3 could be due to the formation of hydrogen bond as well as the π–π interaction between the MO molecules and PANI (Van der Waals forces) (Janaki et al., 2012). For pH value between 4 and 8, the adsorption capacity was at its maximum value (about 20 mg g^{-1}). Under this condition, the surface of PANI was positively charged, since it still existed in the ES form. However, MO molecules now exist dominantly in the anionic form. Therefore, adsorption occurred well within this pH range due to the electrostatic attraction between MO molecules and PANI in addition, it could also be due to the ion-exchange mechanism (Ansari et al., 2011) which explained the chemisorption nature of MO by the immobilized PANI. When the pH was increased to pH 9, PANI underwent transition from ES to EB form. At this stage, the electrostatic attraction ceased to exist. As the pH was increased, adsorption decreased further due to the competition against the excess OH– ions which reduced the interactions between the adsorbent and PANI. Once again, the limited adsorption at high pH values was due to the formation of hydrogen bonds and Van der Waals forces between the adsorbent and the adsorbent.

Fig 8 provides results of the time equilibrium studies for the adsorption of different concentrations of MO by PANI/glass. The adsorption was rapid in the first 15 min due to the surface adsorption, which indicates maximum efficiency, and this behavior is normally associated with physical adsorption or strong chemisorptions (Mahanta et al., 2008). Apparently, the equilibrium time was faster at lower concentrations where its value was 30 min for 5 mg L^{-1} while it required 45 min for both 15 and 30 mg L^{-1} solutions to reach equilibrium. Fig. 8 also provides the time equilibrium plot for PANI powder

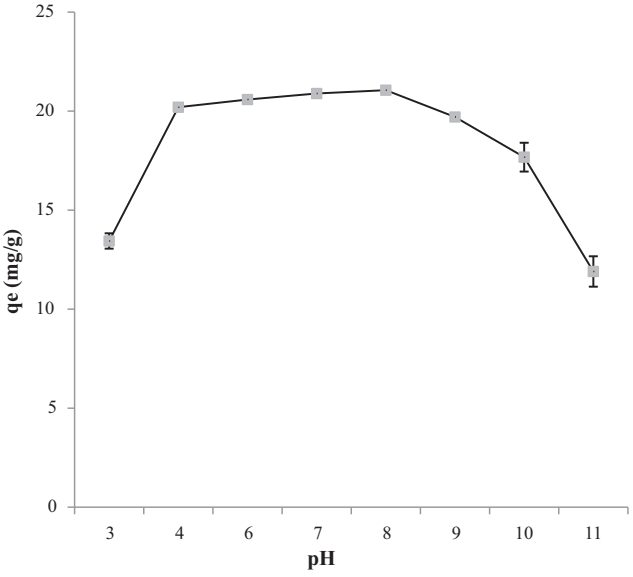

Figure 7 Effect of pH on the adsorption capacity of MO onto PANI/glass [V: 0.02 L, t: 90 min, m: 1.41 mg cm^{-2}, C_o: 20 mg L^{-1}, and T: 29 °C].

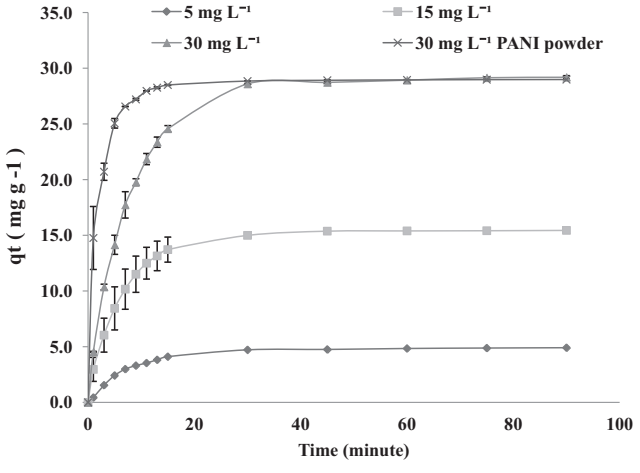

Figure 8 Effect of contact time on the adsorption capacity of MO by PANI powder and PANI/glass at various initial concentrations of MO [V: 0.02 L, t: 90 min, pH: solution (7.0), m: 1.41 mg cm^{-2} and T: 29 °C].

where it took only 15 min to reach the equilibrium state. Interestingly q_e obtained for PANI powder (suspended mode) was 29 mg g^{-1} which was only slightly higher than the q_e (27 mg g^{-1}) for the immobilized PANI/glass. The reason for the relatively high q_e value obtained for the immobilized system was due to the netlike nature of its surface as described earlier whereby it allowed the penetration of solution into the lower layer of the immobilized PANI. However, it can be said that immobilization of adsorbent tends to slow down the mass transport of the dye toward the PANI particles. This is obvious by comparing the equilibrium time attained for the suspended mode and the immobilized mode and also the longer time taken for the solutions with higher concentrations to attain equilibrium as indicated in Fig. 8. As with the case of immobilized chitosan (Nawi et al., 2010), a longer equilibrium time was needed for higher dye concentrations as there was a tendency for the adsorbate to penetrate deeper within the interior surface of the PANI/glass system and this diffusion of dye molecules toward the deeper sub-layer of PANI/glass was a relatively slow process. While the effect of the initial concentrations on the attainment of equilibrium state shows similar trend as the suspended systems (Ansari and Mosayebzadeh, 2011; Gemeay et al., 2008) the impact however was more drastic for the immobilized system.

3.3. Adsorption isotherms

The Langmuir isotherm model is based on the assumption of a monolayer adsorption, where all the sorption sites are identical and energetically equivalent (Mittal et al., 2007). The linearized Langmuir isotherm can be expressed by the equation below:

$$\frac{C_e}{q_e} = \frac{1}{K_L} + \frac{a_L}{K_L} C_e \tag{3}$$

where C_e is the concentration of MO at equilibrium in the liquid phase (mg L^{-1}), q_e is the adsorption capacity at equilibrium (mg g^{-1}), K_L and a_L is the Langmuir isotherm constant in L g^{-1} and L mg^{-1}, respectively. K_L and a_L can be calculated from the intercept and slope of plot C_e/q_e versus C_e. The maximum adsorption capacity of PANI/glass (q_{max}) is numerically equal to K_L/a_L. The Freundlich isotherm on the other hand explains the adsorption on a heterogeneous surface with uniform energy and there are interactions between the adsorbed molecules. This means that it is not restricted to the formation of a monolayer. The linearized Freundlich isotherm can be described as follows:

$$\ln q_e = \ln K_F + \frac{1}{n_F} \ln C_e \tag{4}$$

where q_e is the adsorption capacity at equilibrium (mg g^{-1}), C_e is the MO concentration at equilibrium in the liquid phase (mg L^{-1}), K_F and n_F are the Freundlich constant related to the bonding energy (L g^{-1}) and adsorption intensity or surface heterogeneity, respectively. K_F and n_F can be calculated from the intercept and slope of plot $\ln q_e$ versus $\ln C_e$.

The Langmuir and Freundlich adsorption isotherm data for both immobilized PANI/glass and PANI powder are summarized in Table 1 while the Langmuir and Freundlich plots are given in Supplementary Fig. 3. Based on the obtained coefficient of determination (R^2), the suspended powder system obeys Langmuir isotherm better than Freundlich model while the immobilized system follows Freundlich better than Langmuir model. Other reports involving PANI powder as adsorbents (Ayad and Abu El Nasr, 2010; Salem, 2010; Samani et al., 2010; Cui et al., 2012; Ayad et al., 2012) indicated the same tendency for the suspended powder system to follow Langmuir model. In other words, surface heterogeneity is more pronounced when the adsorbent is immobilized on a flat surface. Table 2 provides the comparison of q_{max} values from this study and the reported literatures involving adsorption of MO by PANI (Ai et al., 2010; Salem, 2010) and other adsorbents (Drelinkiewicz et al., 2005; Shiue et al., 2012) used in suspended particles and PANI in immobilized mode (this study). The q_{max} for PANI/glass and PANI powder was 92 mg g^{-1} and 147 mg g^{-1}, respectively. Although the suspended PANI system exhibits higher removal efficiency, the requirement of the filtration unit for separating the treated water and recovering PANI powder can be tedious and can increase the overall costs of the treatment process. Therefore, immobilizing PANI on flat surfaces such as glass plates (PANI/glass) is proven here to be an effective adsorbent with the added convenience of direct discharge of the treated water and easy recovery of the adsorbent and its reuse.

From the adsorption isotherm data at different temperatures, thermodynamic parameters, such as, Gibb's free energy (ΔG°), the entropy (ΔS°) and the enthalpy (ΔH°) can be obtained using the following relations.

$$K_c = \frac{C_{Ae}}{C_e} \tag{5}$$

$$\Delta G^\circ = -RT \ln K_C \tag{6}$$

$$\log K_c = -\frac{\Delta S^\circ}{2.303\mathrm{R}} + \frac{\Delta H^\circ}{2.303\mathrm{R}T} \tag{7}$$

where, K_c is the equilibrium constant, C_{Ae} is the amount of dye adsorbed on solid at equilibrium (mg L^{-1}), C_e is the equilibrium concentration of dye in the solution (mg L^{-1}), R is the gas constant (8.314 J mol^{-1} K^{-1}) and T is the temperature in

Table 2 Comparison of maximum adsorption capacities (q_{max}) for MO on various adsorbents with present study.

Adsorbents	q_{max} (mg g^{-1})	References
PANI microsphere	154	Ai et al. (2010)
Hypercrosslinked polymer	76.9	Huang et al. (2008b)
Copper oxide	1.2	Shiue et al. (2012)
Ammonium-functionalized MCM-41	1.12	Qin et al. (2009)
PANI coated sawdust	99	Ansari and Mosayebzadeh (2011)
PANI/glass	93	Present study
PANI powder	147	Present study

Kelvin (Nawi et al., 2010). From the van't Hoff plots of $\ln K_c$ versus $1/T$ (see Supplementary Fig. 4), the values of $\Delta H°$ and $\Delta S°$ can be calculated from the slope and the intercept (Huang et al., 2008a,b). Table 3 lists the calculated thermodynamic parameters for both immobilized and suspended PANI systems in the adsorption of MO. The increasing negative values of $\Delta G°$ with temperature for immobilized PANI suggest that the process is less favored at higher temperatures and is spontaneous. In addition, the considerably low $\Delta G°$ values illustrate the saturation of the adsorption process. On the other hand, the negative value of $\Delta H°$ indicates that the adsorption process is an exothermic process and thus is less favorable at higher temperatures. This is supported by the fact that $\Delta G°$ increased with increasing temperature. Furthermore, the negative value of $\Delta S°$ for PANI/glass shows that the randomness at the solid PANI/MO solution interface decreases during the adsorption of MO onto the PANI/glass system. A similar observation was indicated by (Nawi et al., 2010) for the adsorption of reactive red 4 dye by the immobilized chitosan on a glass plate. On the other hand, the adsorption of MO by suspended PANI powder was endothermic and with positive entropy. Clearly, the thermodynamic data for the immobilized system seemed to be different from the conventional suspended system whereby in most cases the adsorption was endothermic with positive $\Delta S°$ values (Ai et al., 2010; Karthikeyan et al., 2009). The randomness is expected to decrease for the immobilized system because of the fixed flat layered arrangement of the adsorbent on the glass plate.

3.4. Adsorption kinetics

In order to investigate the controlling mechanism of the adsorption processes of MO dye by PANI powder and immobilized PANI/glass, the pseudo-first order, pseudo-second order and intraparticle diffusion models were employed for interpreting the adsorption data. The respective equations for pseudo-first-order (Abramian and El-Rassy, 2009), pseudo-second-order (Cestari et al., 2004) and intraparticle diffusion models are as shown below:

$$\ln(q_e - q_t) = \ln q_e - k_1 t \tag{8}$$

$$\frac{t}{q_t} = \frac{t}{q_e} + \frac{1}{k_2 q_e^2} \tag{9}$$

$$q_t = k_i\, t^{0.5} + C \tag{10}$$

$$q_t = b + a \ln t \tag{11}$$

where q_e and q_t are the amounts of dye adsorbed (mg g^{-1}) at equilibrium and at time t (min), and t is the adsorption time (min). For the intraparticle equation (Eq. (10)), k_i is the intraparticle diffusion rate constant in mol g^{-1} $min^{-0.5}$ and C is an intercept (mol g^{-1}) which is proportional to the boundary layer thickness. The larger the C value, the greater is the boundary layer effect (Nethajia et al., 2010). The other parameters are different kinetics constants that can be determined by the slope of the experimental data. The corresponding kinetic parameters and the correlation coefficients are summarized in Table 4. Apparently, the pseudo-first-order kinetic model did not fit well to model the adsorption kinetics of both suspended and immobilized PANI system since the calculated adsorption capacity value ($q_{e,\mathrm{cal}}$) was different from the experimental data ($q_{e,\mathrm{exp}}$). In addition, the coefficient of determination (R^2) ~ 0.968 was relatively poor. In contrast, the coefficient of determination (R^2) for the second-order kinetics model was $\geqslant 0.998$ and the $q_{e,\mathrm{cal}}$ value was in better agreement with the $q_{e,\mathrm{exp}}$ value. Therefore, both immobilized and suspended PANI systems follow pseudo second order kinetics. This

Table 3 Comparison in thermodynamic parameters for the adsorption of Methyl Orange in PANI powder and PANI/glass [V: 0.02 L, t: 60 min, m: 0.94 mg cm^{-2}, 20 mg, C_o: 20 mg/L, and T: 29 °C].

T (K)	PANI/glass			PANI powder		
	$\Delta G°$ (kJ mol^{-1})	$\Delta H°$ (kJ mol^{-1})	$\Delta S°$ (J mol^{-1} K^{-1})	$\Delta G°$ (kJ mol^{-1})	$\Delta H°$ (kJ mol^{-1})	$\Delta S°$ (J mol^{-1} K^{-1})
300	−10.50	−25.26	−49.24	−6.56	20.72	91.12
320	−9.47			−8.56		
340	−8.54			−10.19		

Table 4 Kinetic parameters for the adsorption of MO onto PANI powder and PANI/glass [V: 0.02 L, t: 60 min, m: 0.94 mg cm^{-2} (or 20 mg by weight), C_o: 30 mg/L, and T: 29 °C].

Kinetic models	Parameters	PANI powder	PANI/glass
Pseudo-first-order	K_1 (min^{-1})	0.133	0.083
	$q_{e,\mathrm{cal}}$ (mg g^{-1})	7.1	19
	$q_{e,\mathrm{exp}}$ (mg g^{-1})	29	29
Pseudo-second-order	R^2	0.918	0.968
	K_2 (g mg^{-1} min^{-1})	0.039	0.006
	$q_{e,\mathrm{cal}}$ (mg g^{-1})	29.4	31.60
	R^2	0.999	0.998
Intraparticle diffusion (for 30 mg L^{-1} MO)	K_i (mg g^{-1} $min^{-0.5}$)	(1) 0.089	(1) 0.158
	R^2	0.984	0.989
	C (mmol g^{-1} min)	7.667	0.000

conclusion is in line with the observed kinetics of most adsorbents (Qin et al., 2009; Dogan et al., 2009; Ayad et al., 2012).

As indicated by Eq. (10), if intraparticle diffusion model operates efficiently then the plot of q_t versus $t^{0.5}$ should be linear. In addition, if the plot passes through the origin, the intraparticle diffusion is then the sole rate-controlling step (Ayad et al., 2012; Huang et al., 2008a,b; Nethajia et al., 2010). On the other hand, if the intercept deviates from the origin, the importance of the external film resistance cannot be ignored (Karthikeyan et al., 2009). Based on Fig. 9, the plot of q_t versus $t^{0.5}$ for immobilized PANI was divided into a two-step adsorption process. The first portion is the gradual adsorption stage and the second portion is the final equilibrium stage. Based on this analysis, it was found that intraparticle diffusion occurred during the adsorption process due to the relatively high R^2 obtained for the first stage (see Table 4). In addition the straight lines for the immobilized PANI system passed through the origin which could mean that external film resistance was not involved in the rate determining step and therefore the intraparticle diffusion can be accepted as the only rate determining step for the adsorption process. The plot for the suspended particle system is also made up of two stages. However, the straight line for the first stage did not pass through the origin indicating that external film resistance may be a part of the rate determining step besides the intraparticle diffusion. Based on the C value, this external film boundary layer thickness was quiet significant. The observation for the suspended powder PANI system is actually in line with the observation of other published literatures (Ayad et al., 2012; Bhaumik et al., 2012; Ahmed et al., 2016).

As proven earlier, the adsorption of MO molecules by the immobilized PANI adsorbent followed pseudo second order kinetics. Using Eq. (9), plots of (t/q_t) vs t for the adsorption of MO by various loadings or the thickness of immobilized PANI produced straight lines as shown in Supplementary Fig. 5. Some pseudo second order kinetic parameters extracted from the linear plots are provided in Supplementary Table 1. It was observed that an increase in the loading or thickness of the immobilized PANI leads to an increase in the adsorption rate constant, reflecting a fast adsorption process as the thickness increases. This may be because MO molecules can easily find the active sites on the adsorbent surface at higher loadings of the immobilized PANI adsorbent. The initial adsorption rates h (mg g^{-1} min^{-1}) can be calculated from the pseudo-second-order model by the following equation:

$$h = k_{(2)} q_e^2 \tag{12}$$

It was found that the initial rate of adsorption increased with increased loading of the immobilized PANI. This would be expected due to the increase in the driving force due to the higher availability of the active sites at higher adsorbent loadings. This observation provides further evidence that the macropores within the network like structures of the immobilized PANI helped in allowing the efficient mass transport of MO molecules within the immobilized layer.

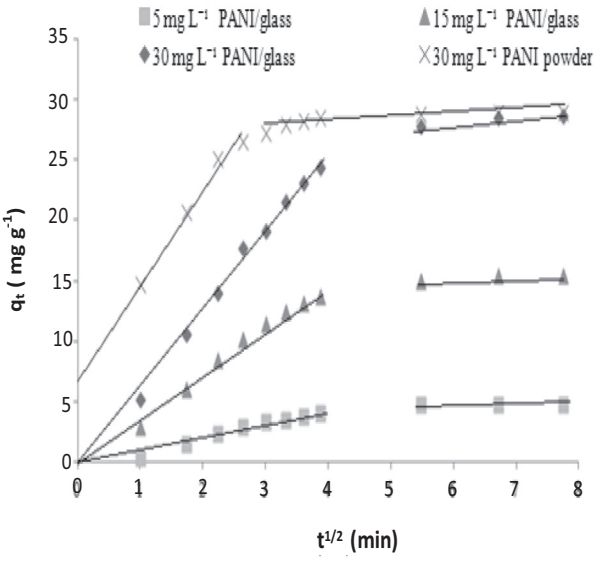

Figure 9 Intraparticle diffusion kinetic plot for the adsorption of MO onto PANI powder and PANI/glass.

3.5. Recyclability and regeneration of the immobilized PANI/glass plate

The advantages of using the immobilized adsorbent system are the convenience of separating the treated water for direct discharge and the recovery of the adsorbent for further reuse. In all cases in this study, the treated solutions were simply discharged out from the reactor, leaving the immobilized adsorbent for further recycling of usage. Most importantly, the saturated immobilized adsorbent could be simply regenerated in situ within the same reactor for regaining its adsorptive efficiency in order to recycle the adsorbent for extended reuse.

As commonly stated by a number of authors (Nawi and Zain, 2012; Mozia et al., 2005; Kodom et al., 2012) the biggest disadvantage of adsorption technique is that it simply involves the transfer of pollutants from the liquid phase to the solid phase. The saturated adsorbent is then conventionally regenerated by desorption of the pollutant back into the liquid phase where in actual fact the pollutant was never really destroyed. In this study, we introduced a novel approach of using the photocatalytic process to regenerate the PANI adsorbent in the hope that the desorbed MO would be directly degraded in situ by the photocatalyst into CO_2 and H_2O. In essence, the pollutant was supposedly destroyed and removed from all the phases involved while the PANI adsorbent was fully regenerated. As stated earlier, desorption of MO occurred under a highly acidic condition. The best photocatalytic activity of TiO_2 for the degradation of azo dyes also occurred under acidic condition (Kodom et al., 2012; Bansal et al., 2010; Huang et al., 2008a,b) while many papers had reported the significant improvement of the photocatalytic process in the presence of H_2O_2 (Mozia et al., 2005; Bansal et al., 2010) These conditions were therefore applied in this study for the photocatalytic regeneration of the saturated PANI plates.

The results of the recycled applications of the immobilized PANI/glass plate for the adsorption of MO and its photocatalytic regeneration are shown in Fig. 10. As shown in Fig. 10a, when the PANI/glass plate was used for the first time, 96% removal of 60 mg L^{-1} MO was achieved. When the same PANI/glass plate was reused again, the uptake of MO as expected decreased due to the reduced adsorption sites. At

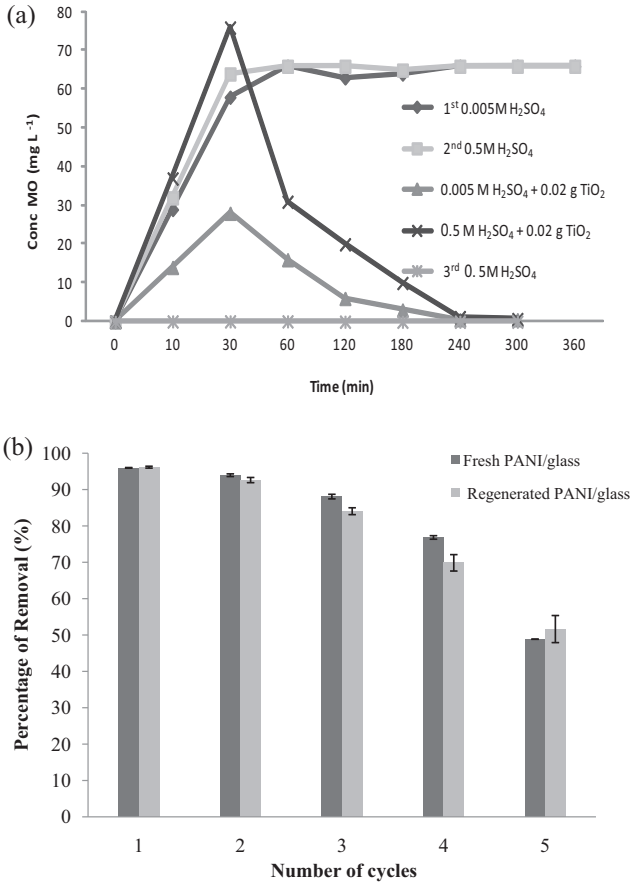

Figure 10 (a) The desorption of MO from the saturated PANI/glass by different concentrations of H_2SO_4 solutions and (b) comparison of percentage removal of MO onto PANI/glass before and after the regeneration process.

the fifth recycled application, 48.9% removal was still achieved by the immobilized PANI.

At acidic pH, PANI would be in its emeraldine salt (ES) form and is positively charged. Therefore MO could be desorbed since in acidic solutions (PH < 2), it was transformed to its cationic form and coulombic charge repulsion would then desorb the dye from the adsorbent into the solution. As shown in Fig. 10b, a partially saturated PANI plate desorbed MO in acidic condition. When a 0.005 M H_2SO_4 was used, desorption of MO continued until the desorbed MO concentration reached 60 mg L^{-1} after which the desorption process ceased to occur due to the equilibrium effect. However, more desorption occurred from the same plate when the solution was changed to a fresh 0.5 M H_2SO_4 solution. The desorption process again ceased when the desorbed MO reached 60 mg L^{-1} due to the similar reason. Therefore it can be concluded that several repetitive applications of fresh solutions of H_2SO_4 are needed in order to completely remove all MO from the PANI/glass plate. Such conventional desorption process is definitely not environment friendly since it merely recycles back the pollutant from the solid phase to the liquid phase without its total destruction.

A viable alternative is to use the photocatalytic approach. It was observed that when the MO saturated PANI/glass plate was photocatalytically regenerated directly with a 0.5 M H_2SO_4 in the presence of TiO_2 and H_2O_2, the system failed to yield colorless solution as expected. This was due to the high MO concentration desorbed within the solution which prevented efficient penetration of light for proper photocatalysis to occur. Therefore in order to solve this problem a two step process was used instead. In the first step involving the 0.005 M H_2SO_4, the concentration of MO at first increased with contact time up to 30 min and then rapidly decreased to almost zero value upon 240 min of irradiation (see Fig. 10b). When the same plate was again irradiated in 0.05 M H_2SO_4 in the presence of TiO_2 and H_2O_2, more MO desorption occurred that increased with time up to 30 min of contact time and once again decreased rapidly beyond this time to reach zero concentration upon 240 min of contact time. The decreasing concentration of MO in the acidic solution observed here was due to the continuous removal of the dye via the photocatalytic process thus avoiding the effect of equilibrium as observed earlier with the simple desorption process. In order to ensure that all MO was desorbed from the plate, the treated PANI/glass plate was soaked inside 0.5 M H_2SO_4. As shown in Fig. 10b, no detection of MO was observed indicating that the PANI/glass plate was completely regenerated. The PANI/glass plate was then removed from the reactor while the solution was irradiated for another 4 h in order to achieve complete mineralization of the dye whereby the total organic carbon (TOC) value of the final solution was zero. In this respect, the novel photocatalytic regeneration approach that has been applied here offered an excellent environment friendly process with no toxic waste generated where the treated acidic solution was neutralized with NaOH and eventually safe to be discharged into the drain.

The adsorption capacity for the regenerated PANI/glass was again tested under similar conditions for the adsorption of MO and the results are shown in Fig. 10a. Apparently, a complete regeneration was achieved since the performance of the generated plate was generally as good as the fresh PANI plate. These preliminary results involving the environment friendly photocatalytic regeneration of the immobilized adsorbent certainly indicate promising potential and we are now currently studying this approach in much greater detail and the comprehensive results will be provided in our future contribution.

4. Conclusion

The immobilized PANI/glass was successfully fabricated using the added PVP during its synthesis as the binder. DRS result reveals that the prepared immobilized PANI was in doped state. Immobilization of PANI powder reduced its BET surface area from 11.8 to 3.7 $m^2 g^{-1}$. SEM micrograph indicates that PANI/glass exhibits a netlike macro porous state which provides a path for the insertion and extraction of molecules or ions. The q_{max} for PANI/glass was 92 mg g^{-1} while the q_{max} of PANI powder was 147 mg g^{-1}. The study also proved that adsorption of MO by PANI/glass improved with aeration where the optimum rate was 40 ml min^{-1}. The optimum pH of adsorption was in the range of 4–8 while the optimum PANI loading was 1.14 mg cm^{-2}. The suspended system obeys Langmuir isotherm model while the PANI/glass system follows Freundlich model. Therefore surface heterogeneity is more pronounced when the adsorbent is immobilized on a flat

surface. The adsorption process for immobilized PANI/glass was less favored at higher temperatures and is an exothermic process. In direct contrast to the PANI powder whose ΔS° values are positive, the immobilized PANI yielded a negative ΔS° value indicating the significant decrease in its randomness. Both immobilized and PANI powder systems follow pseudo second order kinetics. The intraparticle diffusion was the sole rate determining step for the adsorption process of MO by PANI/glass while for the PANI powder system, external film resistance may be a part of the rate determining step besides the intraparticle diffusion. Finally, the immobilized PANI/glass was proven to be highly reusable and can be easily regenerated using a novel photocatalytic process with excellent results. A complete mineralization was achieved for the desorbed MO while the PANI/glass was also fully regenerated. We are now currently studying this approach in much greater detail for use in generating various types of immobilized adsorbents and the comprehensive results will be provided in our future contribution.

Acknowledgements

We would like to thank the Ministry of Education – Malaysia for providing generous financial support under FRGS Grant to conduct this study and the Universiti Sains Malaysia – Malaysia for providing all the needed facilities.

Appendix A. Supplementary data

Supplementary data associated with this article can be found, in the online version, at http://dx.doi.org/10.1016/j.arabjc.2014.10.010.

References

Abramian, L., El-Rassy, H., 2009. Adsorption kinetics and thermodynamics of azo-dye orange II onto highly porous titania aerogel. Chem. Eng. J. 150, 403–410.

Ahmed, S.M., El-Dib, F.I., El-Gendy, N.Sh., Sayed, W.M., El-Khodary, M., 2016. A kinetic study for the removal of anionic sulphonated dye from aqueous solution using nano-polyaniline and Baker's yeast. Arab. J. Chem. 9, S1721–S1728.

Ai, L., Jiang, J., Zhang, R., 2010. Uniform polyaniline microspheres: a novel adsorbent for dye removal from aqueous solution. Synth. Met. 160, 762–767.

Annadurai, G., Juang, R.-S., Lee, D.-J., 2002. Use of cellulose-based wastes for adsorption of dyes from aqueous solutions. J. Hazard. Mater. 92, 263–274.

Ansari, R., Mosayebzadeh, Z., 2011. Application of polyaniline as an efficient and novel adsorbent for azo dyes removal from textile wastewaters. Chem. Pap. 65, 1–8.

Ansari, R., Keivani, M.B., Delavar, A.F., 2011. Application of polyaniline nanolayer composite for removal of tartrazine dye from aqueous solutions. J. Polym. Res. 18, 1931–1939.

Ayad, M.M., Abu El Nasr, A., 2010. Adsorption of cationic dye (Methylene Blue) from water using polyaniline nanotubes base. J. Phys. Chem. C 114, 14377–14383.

Ayad, M.M., Abu El-Nasr, A., Stejskal, J., 2012. Kinetics and isotherm studies of methylene blue adsorption onto polyaniline nanotubes base/silica composite. J. Ind. Eng. Chem. 18, 1964–1969.

Bansal, P., Singh, D., Sud, D., 2010. Photocatalytic degradation of azo dye in aqueous TiO_2 suspension: Reaction pathway and identification of intermediates products by LC/MS. Sep. Purif. Technol. 72, 357–365.

Bhadra, S., Khastgir, D., Singha, N.K., Lee, J.H., 2009. Progress in preparation, processing and applications of polyaniline. Adv. Polym. Technol. 34, 783–810.

Bhaumik, M., Maity, A., Srinivasu, V.V., Onyango, M.S., 2012. Removal of hexavalent chromium from aqueous solution using polypyrrole–polyaniline nanofibers. Chem. Eng. J. 181–182, 323–333.

Blinova, N.V., Sapurina, I., Klimovic, J., Stejskal, J., 2005. The chemical and colloidal stability of polyaniline dispersions. Polym. Degrad. Stab. 88, 428–434.

Cestari, A.R., Vieira, E.F.S., dos Santos, A.G.P., Mota, J.A., de Almeida, V.P., 2004. Adsorption of anionic dyes on chitosan beads. 1. The influence of the chemical structures of dyes and temperature on the adsorption kinetics. J. Colloid Interf. Sci. 280, 380–386.

Chen, J.H., Liu, Q.L., Hu, S.R., Ni, J.C., He, Y.S., 2011. Adsorption mechanism of Cu(II) ions from aqueous solution by glutaraldehyde crosslinked humic acid-immobilized sodium alginate porous membrane adsorbent. Chem. Eng. J. 173, 511–519.

Choudhury, A., 2009. Polyaniline/silver nanocomposites: dielectric properties and ethanol vapour sensitivity. Sens. Actuators, B 138, 318–325.

Comparelli, R., Fanizza, E., Curri, M.L., Cozzoli, P.D., Mascolo, G., Agostiano, A., 2005. UV-induced photocatalytic degradation of azo dyes by organic-capped ZnO nanocrystals immobilized onto substrates. Appl. Catal. B 60, 1–11.

Cui, H., Qian, Y., Qin, L., Zhang, Q., Zhai, J., 2012. Adsorption of aqueous Hg (II) by a polyaniline/attapulgite composite. Chem. Eng. J. 211–212, 216–223.

Dogan, M., Abak, H., Alkan, M., 2009. Adsorption of methylene blue onto hazelnut shell: kinetics, mechanism and activation parameters. J. Hazard. Mater. 164, 172–181.

Drelinkiewicz, A., Waksmundzka, A., Makowski, W., Stejskal, J., 2005. Pd/polyaniline(SiO_2) a novel catalyst for the hydrogenation of 2-ethylanthraquinone. Catal. Commun. 6, 347–356.

Eisazadeh, H., Hojjatinia, K., Ghorbani, M., 2010. Studying the effect of pH on the removal of dichromate from aqueous solution using polyaniline nanocomposites. Health Environ. J. 1, 54–57.

Feng, X., Liu, Y., Lu, C., Hou, W., Zhu, J.-J., 2006. One-step synthesis of AgCl/polyaniline core–shell composites with enhanced electroactivity. Nanotechnology, 173578–173583.

Gemeay, A.H., El-Sharkawy, R.G., Mansour, I.A., Zaki, A.B., 2008. Catalytic activity of polyaniline/MnO_2 composites towards the oxidative decolorization of organic dyes. Appl. Catal. B 80, 106–115.

He, Y., 2005. Preparation of polyaniline microspheres with nanostructured surfaces by a solids-stabilized emulsion. Mater. Lett. 59, 2133–2136.

Huang, M., Xu, C., Wu, Z., Huang, Y., Lin, J., Wu, J., 2008a. Photocatalytic discolorization of methyl orange solution by Pt modified TiO_2 loaded on natural zeolite. Dyes Pigm. 77, 327–334.

Huang, J.-H., Huang, K.-L., Liu, S.-Q., Wang, A.-T., Yan, C., 2008b. Adsorption of Rhodamine B and methyl orange on a hypercrosslinked polymeric adsorbent in aqueous solution. Colloids Surf. A: Physicochem. Eng. Aspects 330, 55–61.

Janaki, V., Byung-Taek, Oh., Vijayaraghavan, K., Kim, J.-W., Ah Kim, S., Ramasamy, A.K., Kamala-Kannan, S., 2012. Application of bacterial extracellular polysaccharides/polyaniline composite for the treatment of Remazol effluent. Carbohydr. Polym. 88, 1002–1008.

Jia, Y., Wang, R., Fane, A.G., Krantz, W.B., 2005. Effect of air bubbling on atrazine adsorption in water by powdered activated carbons – competitive adsorption of impurities. Sep. Purif. Technol. 46, 79–87.

Jia, Y., Wang, b.R., Fane, A.G., 2006. Atrazine adsorption from aqueous solution using powdered activated carbon—improved mass transfer by air bubbling agitation. Chem. Eng. J. 116, 53–59.

Jing, S., Xing, S., Yu, L.Y., Wua, C., 2007. Zhao thesis and characterization of Ag/polyaniline core–shell nanocomposites based on silver nanoparticles colloid. Mater. Lett. 61, 2794–2797.

Karthikeyan, M., Satheesh Kumar, S.S., Elango, K.P., 2009. Conducting polymer/alumina composites as viable adsorbents for the removal of fluoride ions from aqueous solution. Fluorine Chem. 130, 894–901.

Kodom, T., Amouzou, E.G., Djaneye-Boundjou Bawa, L.M., 2012. Photocatalytic discoloration of methyl orange and indigo carmine on TiO_2 (P25) deposited on conducting substrates: effect of H_2O_2 and $S_2O_8^{-2}$. Int. J. Chem. Technol. 4, 45–56.

Krysztafkiewicz, A., Binkowski, S., Jesionowski, T., 2002. Adsorption of dyes on a silica surface. Appl. Surf. Sci. 199, 31–39.

Kumar, P.A., Chakraborty, S., Ray, M., 2008. Removal and recovery of chromium from wastewater using short chain polyaniline synthesized on jute fiber. Chem. Eng. J. 141, 130–140.

Kuramoto, N., Geniès, E.M., 1995. Micellar chemical polymerization of aniline. Synth. Met. 68, 191–194.

Mahanta, D., Madras, G., Radhakrishnan, S., Patil, S., 2008. Adsorption of sulfonated dyes by polyaniline emeraldine salt and its kinetics. J. Phys. Chem. B 112, 10153–10157.

Mansour, M.S., Ossman, M.E., Faraga, H.A., 2011. Removal of Cd (II) ion from waste water by adsorption onto polyaniline coated on sawdust. Desalination 272, 301–305.

Mittal, A., Malviya, A., Kaur, D., Mittal, J., Kurup, L., 2007. Studies on the adsorption kinetics and isotherms for the removal and recovery of methyl range from wastewaters using waste materials. J. Hazard. Mater. 148, 229–240.

Mozia, S., Tomaszewska, M., Morawski, A.W., 2005. Photocatalytic degradation of azo-dye Acid Red 18. Desalination 185, 449–456.

Murugesan, R., Anitha, G., Subramanian, E., 2004. Multi-faceted role of blended poly(vinyl pyrrolidone) leading to remarkable improvement in characteristics of polyaniline emeraldine salt. Mater. Chem. Phys. 85, 184–194.

Nand, A.V., Ray, S., Easteal, A.J., Waterhouse, G.I.N., Gizdavis-Nikolaidis, M., Cooney, R.P., Travas-Sejdic, J., Kilmartin, P.A., 2011. Factors affecting the radical scavenging activity of polyaniline. Synth. Met. 161, 1232–1237.

Nawi, M.A., Zain, Salmiah Md., 2012. Enhancing the surface properties of the immobilized Degussa P-25 TiO_2 for the efficient photocatalytic removal of methylene blue from aqueous solution. Appl. Surf. Sci. 258, 6148–6157.

Nawi, M.A., Sabar, S., Jawad, A.H., Wan Ngah, W.S., 2010. Adsorption of Reactive Red 4 by immobilized chitosan on glass plates: towards the design of immobilized TiO2–chitosan synergistic photocatalyst-adsorption bilayer system. Biochem. Eng. J. 49, 317–325.

Nethajia, S., Sivasamya, A., Thennarasua, G., Saravanan, S., 2010. Adsorption of malachite green dye onto activated carbon derived from *Borassus aethiopum* flower biomass. J. Hazard. Mater. 181, 271–280.

Palaniappan, S., John, A., 2008. Polyaniline materials by emulsion polymerization pathway. Prog. Polym. Sci. 33, 732–758.

Palaniappan, S., Sydulu, S.B., Prasanna, T.L., Srinivas, P., 2011. High-temperature oxidation of aniline to highly ordered polyaniline–sulfate salt with a nanofiber morphology and its use as electrode materials in symmetric supercapacitors. J. Appl. Polym. Sci. 120, 780–788.

Qin, Q., Ma, J., Liu, K., 2009. Adsorption of anionic dyes on ammonium-functionalized MCM-41. J. Hazard. Mater. 162, 133–139.

Ren, L., Li, K., Chen, X., 2009. Soft template method to synthesize polyaniline microtubes doped with methyl orange. Polym. Bull. 63, 15–21.

Sahar, M. Ahmed, Fawzia, I. El-Dib, Nour, Sh. El-Gendy, Waafa, M. Sayed, Mohamed, El-Khodary, 2016. A kinetic study for the removal of anionic sulphonated dye from aqueous solution using nano-polyaniline and Baker's yeast. Arab. J. Chem. 9, S1721–S1728.

Salem, M.A., 2010. The role of polyaniline salts in the removal of direct blue 78 from aqueous solution: a kinetic study. React. Funct. Polym. 70, 707–714.

Samani, M.R., Borghei, S.M., Olad, A., Chaichi, M.J., 2010. Removal of chromium from aqueous solution using polyaniline – poly ethylene glycol composite. J. Hazard. Mater. 184, 248–254.

Shiue, A., Ma, C.-M., Ruan, R.-T., Chang, C.-T., 2012. Adsorption kinetics and isotherms for the removal methyl orange from wastewaters using copper oxide catalyst prepared by the waste printed circuit boards. Sust. Environ. Res. 22, 209–215.

Somani, R.P., 2002. Synthesis and characterization of polyaniline dispersions. Mater. Chem. Phys. 77, 81–85.

Stejskal, J., Gilbert, R.G., 2002. Polyaniline. Preparation of a conducting polymer. Pure Appl. Chem. 74, 857–867.

Sun, Q., Yang, L., 2003. The adsorption of basic dyes from aqueous solution on modified peat–resin particle. Water Res. 37, 1535–1544.

Supri, A.G., Heah, C.Y., 2010. Conductive Polymer Based on Polyaniline-Eggshell Powder (PANI-ESP) composites. Phys. Sci. 21, 81–97.

Weng, C.-H., Pan, Y.-F., 2006. Adsorption characteristics of methylene blue from aqueous solution by sludge ash. Colloids Surf. A 274, 154–162.